SSCL-614

SSCL-614
January 1993
Distribution Category: 414

S. Chen
G. López

Simulation Studies of the Transverse Dipole Mode Multibunch Instability for the SSC Collider

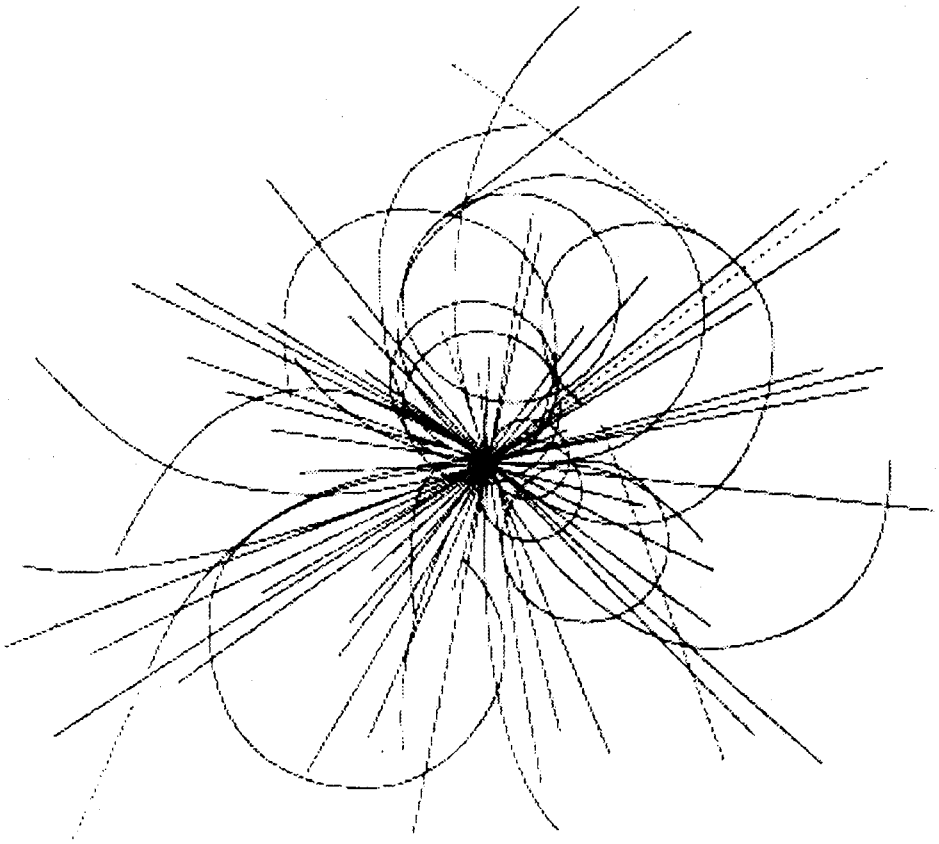

Superconducting Super Collider Laboratory

SSCL-614

Simulation Studies of the Transverse Dipole Mode Multibunch Instability for the SSC Collider

S. Chen and G. López

Superconducting Super Collider Laboratory*
2550 Beckleymeade Avenue
Dallas, TX 75237

January 1993

* Operated by the Universities Research Association, Inc., for the U.S. Department of Energy under Contract No. DE-AC35-89ER40486.

Simulation Studies of the Transverse Dipole Mode Multibunch Instability for the SSC Collider

S. Chen and G. López

Abstract

A computer program that assumes a point-like structure of the bunches, called TADIMMI, has been devised to study the dipole mode multibunch instability in the Superconducting Super Collider (SSC) Collider ring due to a single Positron-Electron Project (PEP) test rf cavity and the resistive wall. For the rf cavity, the following cases are considered: symmetric filling, where good agreement is obtained with ZAP code; nonsymmetric filling; elimination of the most dangerous mode of the cavity; De-Q of the cavity, where a damping ratio is obtained for the cavity; and the feedback system, where it is verified that the proposed system for the Collider will work. For the resistive wall, a resonator impedance model approximation is used, which allows use of the same computer program to study the instabilities and the associated feedback system. Comparison with the analytical approach (ZAP) is also made.

1.0 INTRODUCTION

The SSC Collider will be the first machine operating with 17,424 bunches of protons separated by a relatively short distance,[1] 5 m. The bunches are injected from the High Energy Booster (HEB) into the Collider, which requires eight HEB batches to fill almost symmetrically (there is an abort gap) one of its two rings. The batches are injected into the upper and lower ring one at a time. To inject one batch in the same ring requires a wait of approximately 515 s; the eight batches are injected in approximately 1.14 h. Therefore, there is a great deal of concern about possible multibunch instabilities (longitudinal and transverse) that the beam might suffer during this time. These instabilities are due to the additional electromagnetic forces that a bunch feels because of the wake field created by previous bunches passing by any element of the ring, including beam tube, bellows, rf cavities, scraper, beam position monitors (BPM), kickers (K), *etc.* They can be measured by the time during which the amplitude of the bunch has grown considerably, called "growth time."

Transverse multibunch instabilities are characterized by two different types of motions. The first motion is related to the structure of the bunch itself. For rigidity motion of the bunches, the mode is called *dipole*. For different-shaped oscillations of the bunch, it is called *quadrupole*, *sextupole*, *etc.*, depending on the degree of complexity. The second motion is related to relative oscillations among the bunches; the maximum mode of oscillations is that of the number of bunches.

Quadrupole and higher-order modes of oscillations are expected to be Landau-damped at injection (due to the betatron tune spread, $\sim 10^{-4}$, produced within the bunch by the nonlinear magnetic field at 2 TeV) and during colliding operation (due to the tune spread, $\sim 10^{-3}$, produced within the bunch by the beam-beam interaction at 20 TeV) where, clearly, the frequency shift of the multibunch mode instability is required to be within the betatron tune spread. However, even if these higher-order modes were not Landau-damped, they would be about one order of magnitude less important than the dipole mode.

Two of the most worrisome elements causing transverse instabilities in the Collider are the rf cavity and the resistive wall (beam pipe). Shielded bellows and BPMs in the ring and collimators at the interaction region (IR) do not contribute much to the total transverse impedance of the machine[2] and will be neglected.

The fastest transverse instability at high frequency comes from the rf cavities, and the induced transverse multibunch-mode instability is approximately equal to the number of bunches. Thus, a wide-band feedback system is required in this case to control the instability. We will study this type of instability using the computer program TADIMMI

(Transverse Dipole Mode Multibunch Instability), which uses a point-like structure for the bunches; that is, it restricts itself to study of the dipole-mode (rigid motion of the bunch) multibunch instability,[3] which is the most dangerous of all. We compare the result with the ZAP analytical approach. In addition, we study the following cases: asymmetric filling, elimination of the most dangerous rf-cavity modes, De-Q of the rf cavity, and, finally, the damping feedback system.

The fastest transverse instability at low frequency (the revolution frequency times the fractional part of the tune), on the other hand, is due to the resistive wall.[2] However, a narrow-band feedback system is able to correct this instability. A model for this impedance will be given that allows use of the same program to study this instability and the associated feedback system. In this case, the whole beam pipe will be assumed to be uniform in temperature; we will ignore the West utility warm section, with a total length of approximately 1.3 km. The dimension and the composition of the beam pipe in this region must be chosen carefully so that the resistive wall impedance here does not represent an important contribution to the total resistive wall in the Collider. The elements in this region (scraper, collimators, and kickers) must be copper-coated to reduced inhomogeneous, high transverse impedance values in the ring.

2.0 TADIMMI COMPUTER CODE

Ignoring the possible coupling of different directions in the motion, the transverse amplitude of motion, Y, of a point-like bunch suffering the electromagnetic wake-field interaction, ww, can be described by the differential equation

$$\frac{d^2Y}{dt^2} + \omega_\beta^2 Y = ww \ , \tag{1}$$

where ω_β is the angular betatron frequency. Let us assume the following: for simplicity, there is a single cavity in the ring where there is a point-like interaction, the ring is perfectly linear, and the ring has M equally pair-spaced bunches. With these assumptions the short-range wake field can be omitted, and the long-range is given by the Higher Order Modes (HOM) of the rf cavity. Since the rf cavity is usually much shorter than the betatron wavelength, the betatron phase advance within the rf cavity can be ignored. When the k-bunch passes through the rf cavity for $n+1$ turns, the transverse position does not change:

$$Y(k, n+1) = Y(k, n) \ , \tag{2a}$$

but its momentum is changed by the wake field of the rf cavity.

For dipole-mode wake field, the change in the transverse momentum of the k-bunch is

$$\acute{Y}(k,n+1) = \acute{Y}(k,n) + \frac{Ne^2}{E_o} \sum_{m=1}^{n} \sum_{J=1}^{M} D(j) Y(J,m) W(s/c) \ , \tag{2b}$$

where the summation is carried out over the wake field left behind for all the previous bunches and turns. The variable s can be written in terms of the space between bunches, S_B, as

$$s = (k-J)S_B + (n-m)MS_B \ , \tag{3a}$$

where $(k-J)$ and $(n-m)M$ represent the relative bunch and turn numbers. N is the total number of protons in the bunch, e is the proton charge, E_o is the relativistic energy, $E_o = \gamma mc^2$, c is the speed of light, and $W(s/c)$ is the wake function defined as

$$W(s/c) = \begin{cases} \sum_\lambda A_\lambda \exp(-\alpha_\lambda s/c) \sin(\Omega_\lambda s/c) & \text{if } s > 0 \\ 0 & \text{if } s \leq 0 \ . \end{cases} \tag{3b}$$

The variables A_λ, α_λ, and Ω_λ are defined as

$$A_\lambda = \frac{\omega_\lambda^2}{\Omega_\lambda} \left(\frac{R_\lambda}{Q_\lambda} \right) \ , \tag{3c}$$

$$\alpha_\lambda = \omega_\lambda / 2Q_\lambda \ , \tag{3d}$$

and

$$\Omega_\lambda = \omega_\lambda \sqrt{1 - 1/4Q_\lambda^2} \ , \tag{3e}$$

and the summation is carried out over all the transverse HOMs of the cavity. Each cavity mode is characterized by the resonant angular frequency ω_λ, the shunt impedance R_λ, and the resonant quality factor Q_λ. The quantity

$$\frac{c}{\alpha_\lambda S_B} = \frac{2Q_\lambda c}{\omega_\lambda S_B} \tag{3f}$$

gives us the number of bunches that the exited transverse HOM can affect before it decays by a factor of $1/e$. The factor $D(j)$,

$$0 \leq D(j) = N(j)/N \leq 1 \ ,$$

defines the distribution of bunches and the number of protons per bunch.

The bunch is transported from the output to input of the rf cavity using the Courant-Snyder[4] map:

$$\begin{pmatrix} Y(k,n+1) \\ \acute{Y}(k,n+1) \end{pmatrix} = \begin{pmatrix} \cos\mu + \alpha \sin\mu & \beta \sin\mu \\ -\gamma \sin\nu & \cos\mu - \alpha \sin\mu \end{pmatrix} \begin{pmatrix} Y(k,n) \\ \acute{Y}(k,n) \end{pmatrix} \ , \tag{4}$$

where μ, α, β, and γ are the Courant-Snyder parameters valuated at the cavity location.

The relations (2), (3), and (4) comprise the model for simulating transverse multibunch instabilities with the computer program TADIMMI.

3.0 SYMMETRIC FILLING AND COMPARISON WITH ZAP

A 358.9-MHz Positron-Electron Project (PEP) cavity will be taken as the test cavity in the TADIMMI program. The characteristics of its transverse HOM are shown in Appendix A. The initial distribution of bunches is uniform in the amplitude variable with a maximum amplitude of 1 mm. The statistic weight, $0 \leq D(j) \leq 1$, is random-variable with uniform distribution. At the rf location, the dispersion function is zero, as assumed in Eq. (4), and the Courant-Snyder parameters have the following values:

$$\beta = 112,472.0 \text{ mm} ,$$

$$\alpha = 0 ,$$

and

$$\mu = 2\pi \text{frac}(\nu) = 1.759292 .$$

The characteristics of the bunches are

$$N = 7.5 \times 10^9 ,$$

$$M = 17,424 ,$$

$$E_o = 2 \text{ TeV} ,$$

and

$$S_B = 5 \text{ m} .$$

The case of nonuniform distribution of particles in the bunches $\left(D(j) = Random[0,1]\right)$ will be presented in detail in this section. Figures 1–4 show how the amplitude of different bunches of the beam behave as a function of time (turns). Figure 5 shows the distribution of the bunches in the phase space once the instability has set in. The bunch that leads the amplitude growth may differ from time to time as shown in Figure 6. Finally, from the value of the slope on the curve (maximum amplitude of the bunches as a function of time), the growth time can be calculated. This curve is shown in Figure 7; the estimated growth time is $\tau = 23.8$ s. Table 1 summarizes the growth time calculations for different cases.

The comparison with the analytical approach (ZAP[5]) is shown in Figure 8. The simulation result for uniform distribution $\left(D(j) = 1\right)$ agrees very well with this analytical approach.

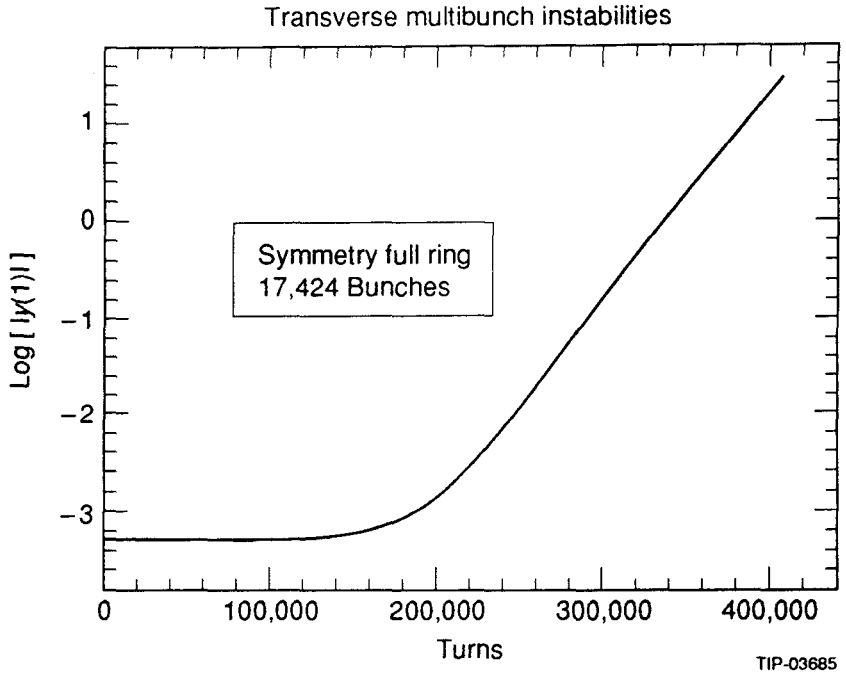

Figure 1. Amplitude Growth of the First Bunch.

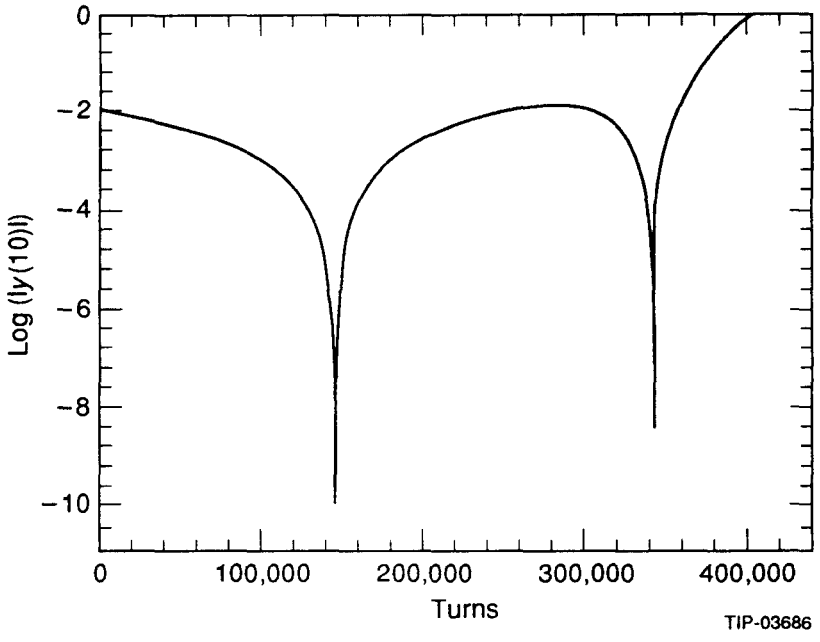

Figure 2. Amplitude Growth of the Tenth Bunch.

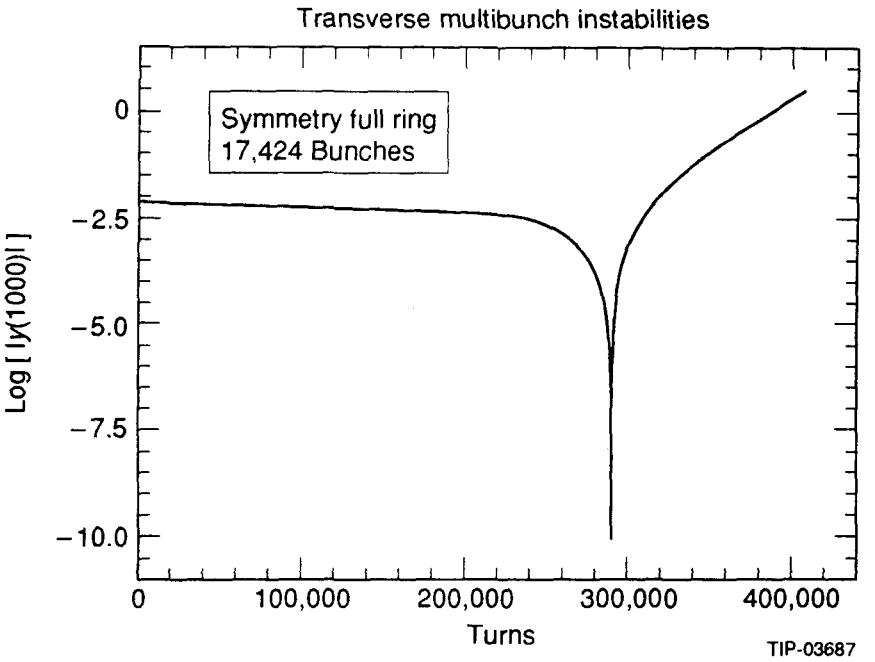

Figure 3. Amplitude Growth of the First Thousand Bunches.

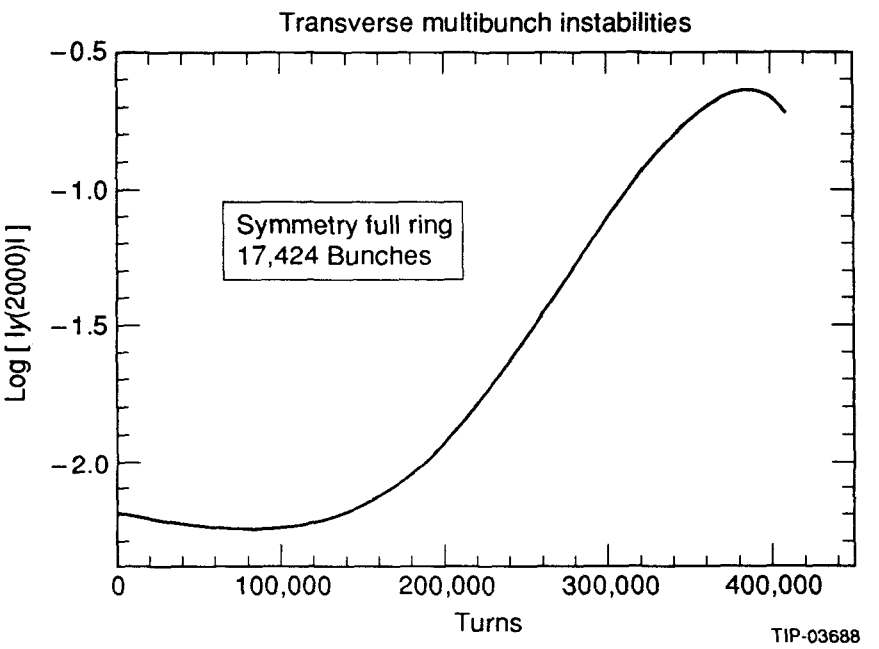

Figure 4. Amplitude Growth of the Second Thousand Bunches.

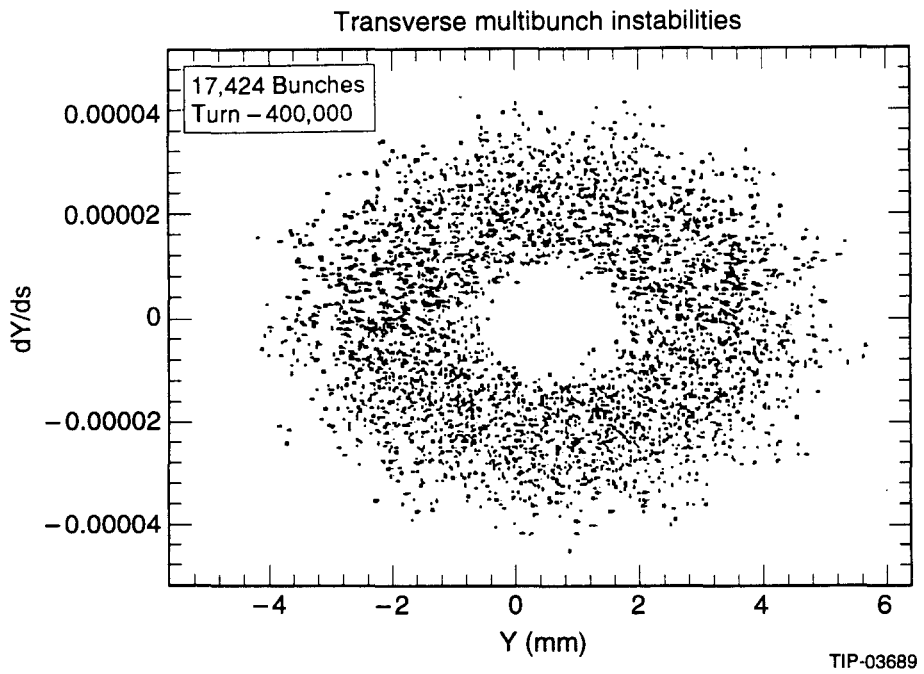

Figure 5. Distribution of the Bunches in the Phase Space.

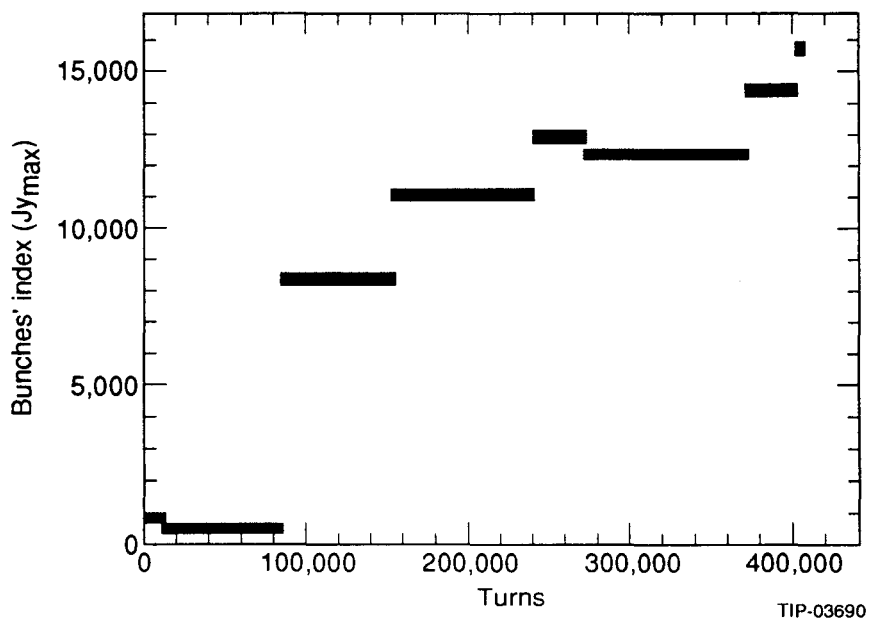

Figure 6. Bunch That Leads the Amplitude Growth.

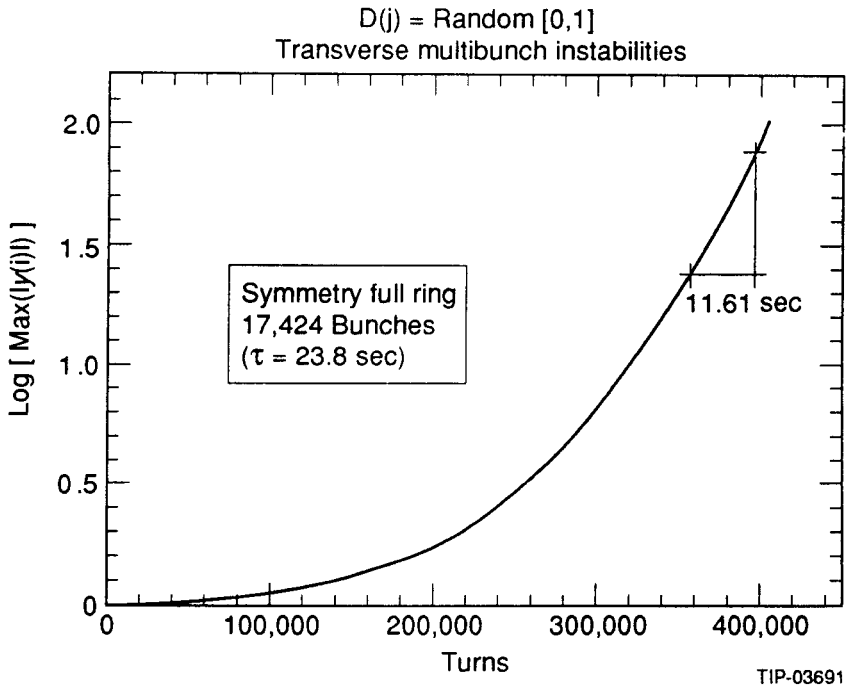

Figure 7. Maximum Amplitude Growth for Growth Time Calculations.

Table 1. Growth Time (s).

$D(j)$	1.0	Random[0,1]
$Y(j)$		
1.0	8.13	15.0
Random[0,1]	8.93	24

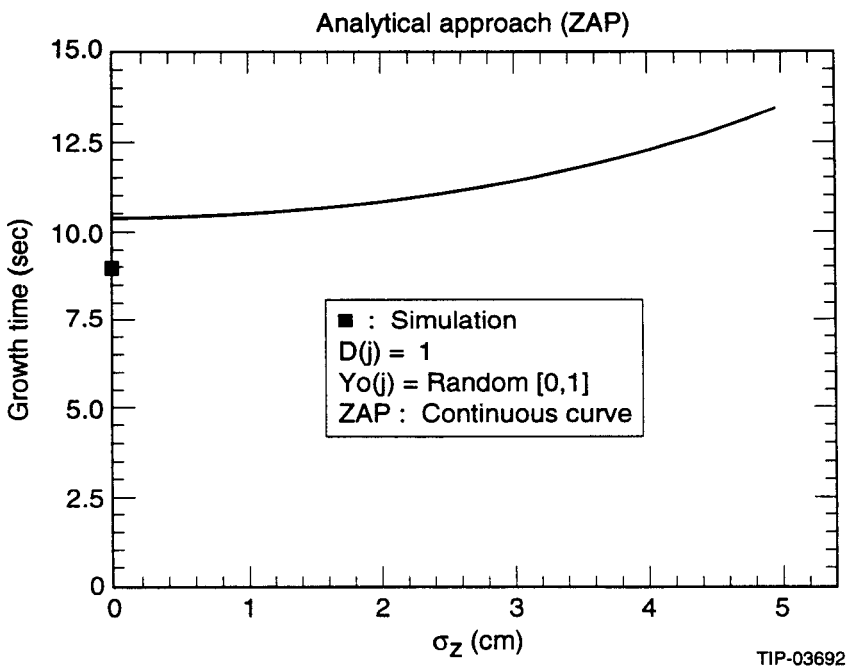

Figure 8. ZAP Growth Time as a Function of the Bunch Length.

4.0 ASYMMETRIC FILLING

A single ring of the Collider is filled from the HEB with eight batches, each with 2178 bunches. This asymmetric state of the ring during filling can be simulated using the above-mentioned variable $D(j)$. For a given number of batches $r < 8$, this function is chosen as

$$D(j) = \begin{cases} \text{Random}[0,1] & \text{if } j \leq r \times 2178 \\ 0 & \text{if otherwise} \end{cases}$$

The result of our calculations can be seen in Figure 9, where the growth time has been plotted as a function of the number of HEB batches. As we can see, the worst situation of the dipole mode multibunch instability occurs in the symmetric filling case. This result verifies the qualitative analytical approach given by Kohaupt[6] for nonsymmetric filling. (See Appendix B.)

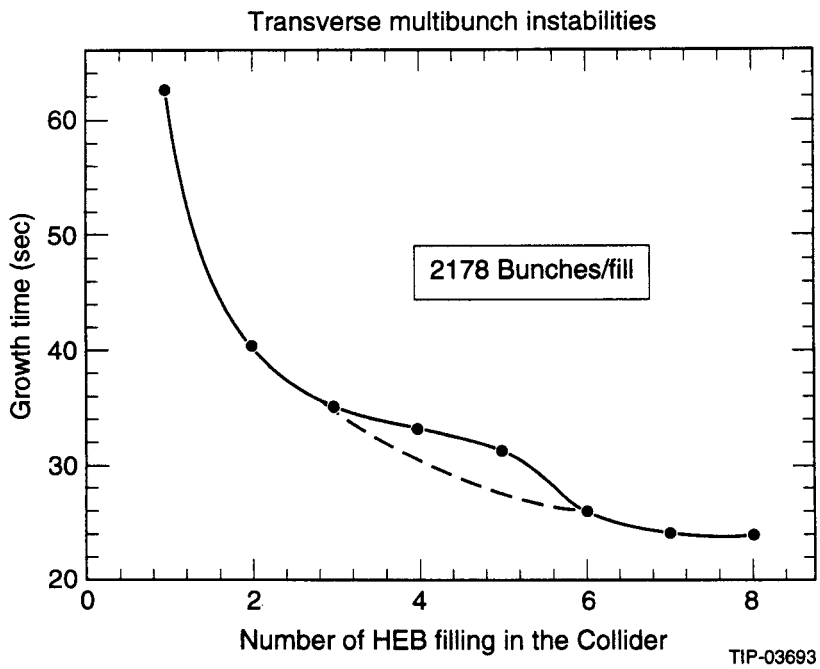

Figure 9. Growth Time as a Function of the Partial Collider Filling.

5.0 PASSIVE DAMPING SYSTEM

One way to increase the growth time of the multibunch instabilities is to eliminate the most dangerous rf HOM and to make a De-Q of the cavity. (Landau damping is not considered.) As we saw in Section 4, the most dangerous situation is the symmetric filling case. Hence, only this case will be considered here.

Assume that some HOMs of the cavity are eliminated to obtain a possibly more stable beam. As Figure 10 shows, if only one mode is eliminated, it does not matter which; the beam, as expected, continues to present the dipole-mode multibunch instability. The bump

appearing in the continuous curve is due to the suppression of the rf-HOM3 (Appendix A), which has the highest value in the quality factor R/Q and higher influence on growth time. The black square marks in Figure 10 represent the growth time for the suppression of several dangerous HOMs of the PEP cavity. As can be seen, even if three of these HOMs remain in the cavity, the dipole-mode multibunch instability continues to be important.

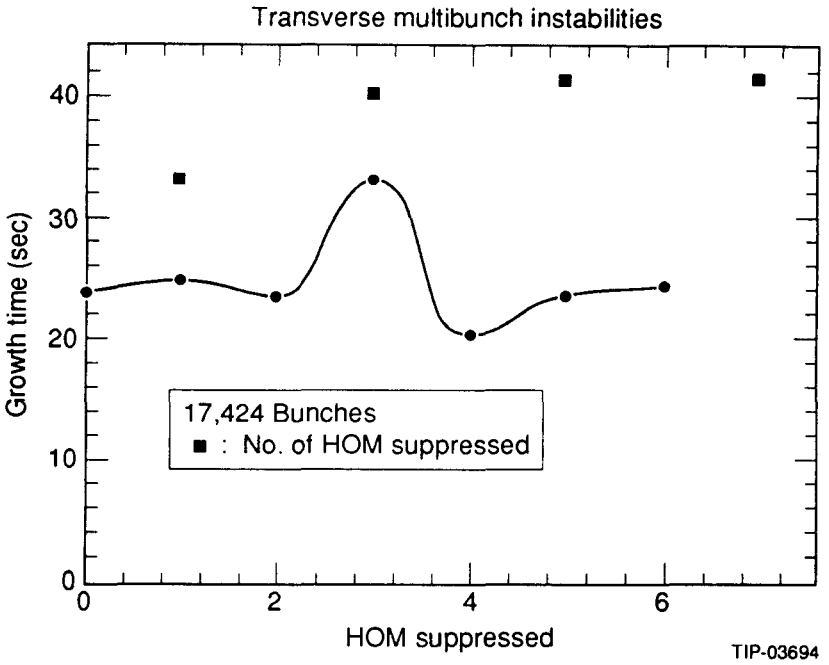

Figure 10. Growth Time as a Function of Suppressed PEP-HOM.

Figure 11 shows the case for a De-Q of the PEP-cavity, *i.e.*, for the case when the Q of all the HOMs of the cavity decrease their value by some given amount, leaving the other quality factor, R/Q, fixed. If this type of cavity is used for the SSC Collider, about 32 single-cell rf cavities would be needed to provide the required power to the beam. Thus, the growth time must be divided by 32 in order to obtain the total dipole-mode instability growth time for the Collider. In addition, a factor of approximately 3 must be considered since, from Table 1, the realistic situation for the Collider is $D(j) = 1$. Doing so in Figure 11, it is seen that for an average value of $R/Q = 125\ \Omega/\mathrm{m}$ and a luminosity of $L = 10^{33}\ \mathrm{cm}^{-2}\mathrm{s}^{-1}$, the following damping factor is required:

$$\frac{Q}{Q_d} \geq 75 \ , \tag{5}$$

or

$$Q_d \leq 1200 \ , \tag{6a}$$

for the growth time to be higher than the injection time, bringing about good stability conditions during this time. To see what happens at a higher luminosity, notice from

Eqs. (2b), (3b), and (3c) that a higher luminosity is equivalent to increasing the quality factor R/Q. Figure 12 shows the effect on the growth time for a decreasing value of this factor, leaving the Q values of the HOM fixed. Putting these two pieces of information together, the following gross estimation can be made to select Q_d, given the number of cavities, N_c:

$$Q_d \leq \frac{4.8 \times 10^6\ \Omega/\mathrm{m}}{< R_\perp/Q > N_c} \ . \tag{6b}$$

A single-cell normal cavity with HOM couplers[7] or a single-cell superconducting (s.c.) cavity with couplers[8] can satisfy this restriction.

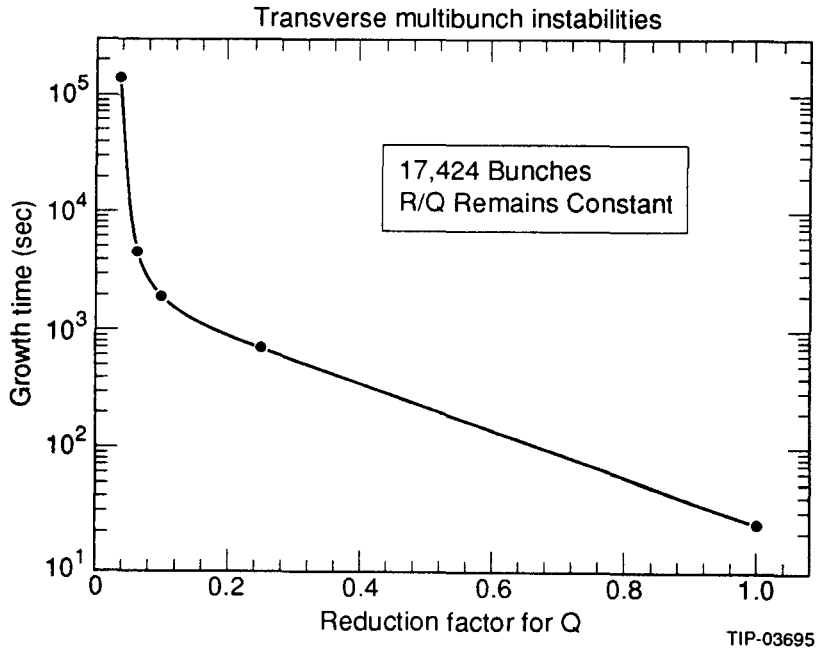

Figure 11. Growth Time as a Function of the De-Q of the PEP Cavity.

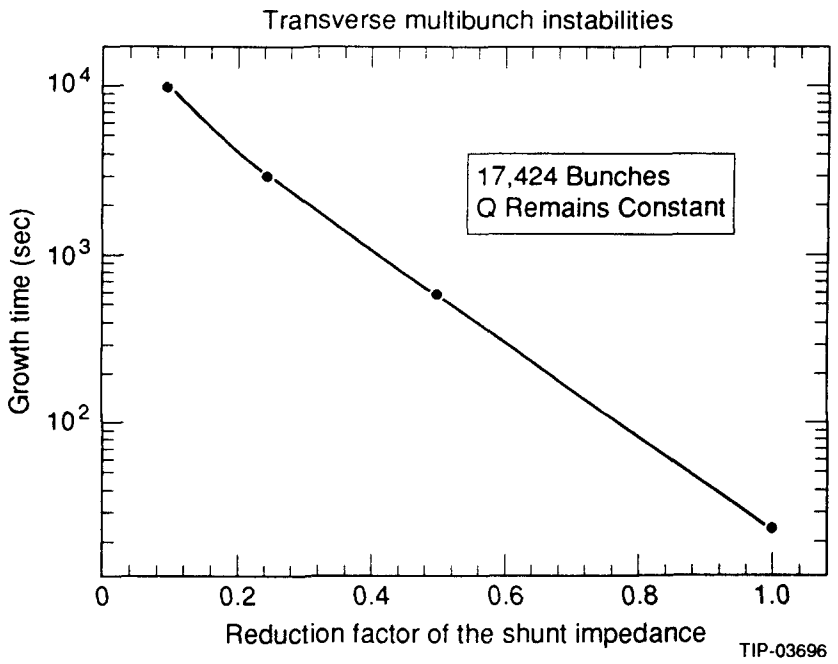

Figure 12. Growth Time as a Function of the De-R/Q of the PEP Cavity.

6.0 ACTIVE DAMPING SYSTEM

Another way to control multibunch instabilities is to use an active feedback system.[9] (Balakin-Novokhatesky-Smirnov, or BNS, damping is ignored.) The SSC Collider will have at least three different feedback systems,[10] one for injection errors, another for the resistive wall, and a third for rf-cavity multibunch instabilities. This last one is the one we are interested in here.

The normal operation of the transverse feedback system uses a BPM to measure the transverse displacement of the bunch. The signal is amplified and transmitted to the kicker (K), located downstream at a phase advance of $\pi/2$ (to optimize the damping rate). This produces an angular deviation to the bunch given by[11]

$$\Delta \acute{Y} = \frac{g}{\sqrt{\beta_{BPM}\beta_K}}(Y_{BPM} + \delta Y) \ , \tag{7}$$

where g is the gain of the system, β_{BPM} and β_K are the beta function at the location of the BPM and the K, and Y_{BPM} and δY are the displacement measured by the BPM and the error transmitted by this displacement. This error is called the resolution of the BPM and is due to the electronic noise in the system.

However, because the protons travel almost at the speed of light, the electronics associated with the feedback system are not fast enough to implement this same-turn scheme.

We have to wait for another turn in order to correct the previous turn (previous-turn scheme). Therefore, both schemes must be studied.

The modification in the program is clear: the kicked bunch in the rf cavity is transported to the BPM, where the information of the displacement is extracted. Then, the bunch is transported to K, where it receives an appropriate kick, depending on the scheme (same-turn or previous-turn). Finally, it is transported to the rf cavity, where it experiences the known rf kick, and so on. The locations of the BPM, K, and rf system in the ring are characterized by (β_1, α_1), (β_2, α_2), and $(\beta_3, 0)$, and they are separated by a phase advance $\pi/2$, μ_2, and μ_3 such that the total phase advance in the machine is $\mu = \mu_3 + \mu_2 + \pi/2$. The matrices that make transport from rf to BPM, from BPM to K, and from K to rf are given by

$$M_1 = \begin{pmatrix} \sqrt{\frac{\beta_1}{\beta_3}}\ \cos\mu_3 & \sqrt{\beta_1\beta_3}\ \sin\mu_3 \\ -\frac{1}{\sqrt{\beta_1\beta_3}}(\sin\mu_3 + \alpha_1\cos\mu_3) & \sqrt{\frac{\beta_3}{\beta_1}}(\cos\mu_3 - \alpha_1\sin\mu_3) \end{pmatrix} \tag{8a}$$

$$M_2 = \begin{pmatrix} \alpha_1\sqrt{\frac{\beta_2}{\beta_1}} & \sqrt{\beta_1\beta_2} \\ -\frac{1+\alpha_1\alpha_2}{\sqrt{\beta_1\beta_2}} & -\alpha_2\sqrt{\frac{\beta_1}{\beta_2}} \end{pmatrix} \tag{8b}$$

and

$$M_3 = \begin{pmatrix} \sqrt{\frac{\beta_3}{\beta_2}}\ (\cos\mu_2 + \alpha_2\sin\mu_2) & \sqrt{\beta_2\beta_3}\ \sin\mu_2 \\ -\frac{1}{\sqrt{\beta_2\beta_3}}(\sin\mu_2 - \alpha_2\cos\mu_2) & \sqrt{\frac{\beta_2}{\beta_3}}\ \cos\mu_2 \end{pmatrix} . \tag{8c}$$

We assume a white noise for the system, with Gaussian distribution for the variable δY having a standard deviation, $\sigma_{\delta Y}$, given by the resolution of the BPM. This Gaussian distribution is obtained with the help of the Central-Limit-Theorem[12] and the distribution

$$\Delta = \sum_{i=1}^{6}(\xi_i - 0.5)\ , \tag{9a}$$

where ξ_i, $i = 1, \ldots, 6$ are random variables having values in the interval [0,1]. Δ has the following characteristics :

$$< \Delta >= 0 \tag{9b}$$

and

$$< \Delta^2 >= 1\ . \tag{9c}$$

Figure 13 shows this distribution. δY is then given by

$$\delta Y = \Delta\sigma_{\delta Y} \ . \tag{10}$$

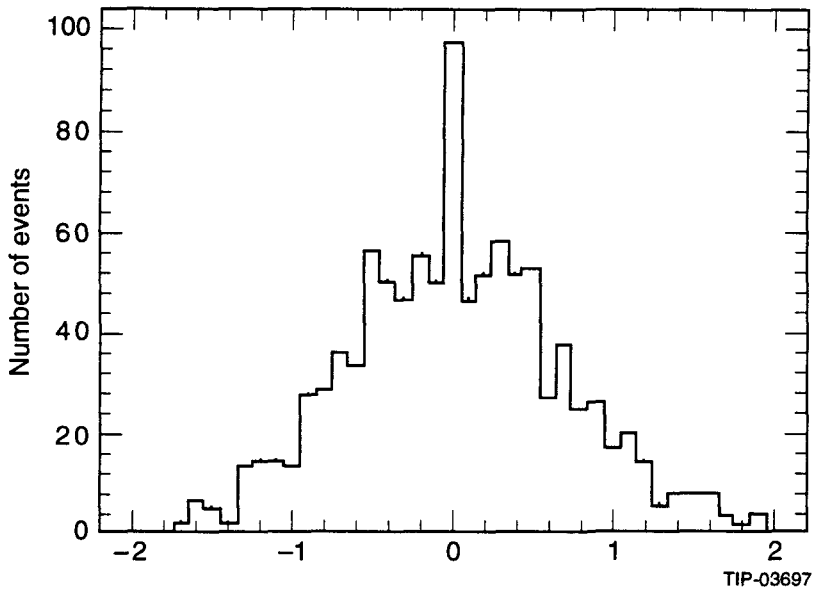

Figure 13. Δ Gaussian Distribution.

The feedback systems will be located at the West Utility section of the Collider ring. Figure 14 shows the beta function behavior at this region and the location of the BPM and K for our simulations. Assume the following characteristics of the feedback system:

$$BW \geq 30 \text{ MHz} \ ,$$

$$\beta_{BPM} = \beta_K \approx 420 \text{ m} \ ,$$

$$g = 0.1 \ ,$$

and

$$\sigma_{\delta Y} = 10 \ \mu\text{m} \ .$$

Figure 15 shows the result for both schemes above and compares them with the no-feedback system seen in Figure 7. As is clearly shown, the simulations suggest that this feedback system will work for damping the transverse dipole-mode multibunch instability. The power required for the kickers can be calculated from the above parameters (see Reference 11). Due to limitations on the CPU time calculations, it is not possible to study the optimization of this feedback system for different noise levels and gains. This study will be done in the near future after the program has been simplified.

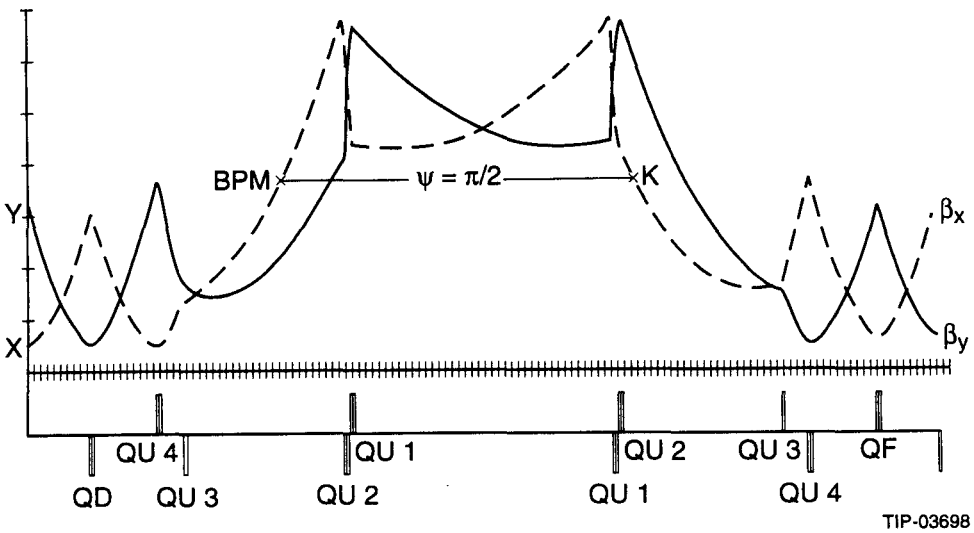

Figure 14. Location of BPM and K in West Utility (Simulations).

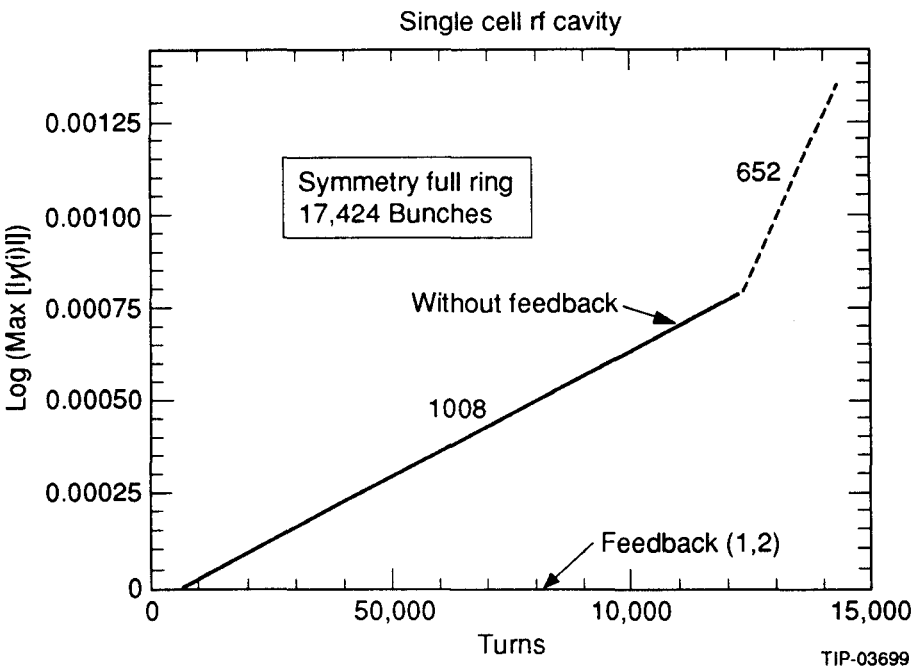

Figure 15. Growth Time Without Feedback, One-Turn-Scheme Feedback and Previous-Turn-Scheme Feedback Schemes (1,2).

7.0 APPROXIMATION OF THE RESISTIVE WALL MULTIBUNCH INSTABILITY

The long-range resistive wall impedance for a stainless steel beam tube coated with copper is given by[1]

$$Z_\perp(\omega) = \frac{\Big(1 - i\sin(\omega)\Big)c\xi(\omega)C}{\pi\omega b^3\sigma_1\delta_1(\omega)}\ , \tag{11}$$

where c is the speed of light, C is the circumference, σ_1 is the copper conductivity, δ_1 is the copper skin depth,

$$\delta_1(\omega) = \sqrt{\frac{2}{\mu_o \sigma_1 \omega}} \ , \tag{12}$$

ξ is a correction factor that takes into account the stainless-steel effect,

$$\xi(\omega) = \frac{1 + \sqrt{\frac{\sigma_2}{\sigma_1}} Z_1(\omega) Z_2(\omega)}{Z_1(\omega) + \sqrt{\sigma_2 \sigma_1}\ Z_2(\omega)} \ , \tag{13a}$$

where σ_2 is the stainless steel conductivity, and Z_1 and Z_2 are given by

$$Z_k(\omega) = \frac{1 - \exp\Big(-(2-i)t_k/\delta_k(\omega)\Big)}{1 + \exp\Big(-(2-i)t_k/\delta_k(\omega)\Big)} \ , \tag{13b}$$

and finally, $\sin\omega$ is the sine function,

$$\sin\omega = \begin{cases} +1, & \text{if } \omega \geq 0 \\ -1, & \text{if } \omega < 0 \end{cases} \ . \tag{14}$$

Figure 16 shows the real part of this impedance for a thickness of 0.1 mm of copper and 1.0 mm of stainless steel, and a beam pipe radius of 1.622 cm.

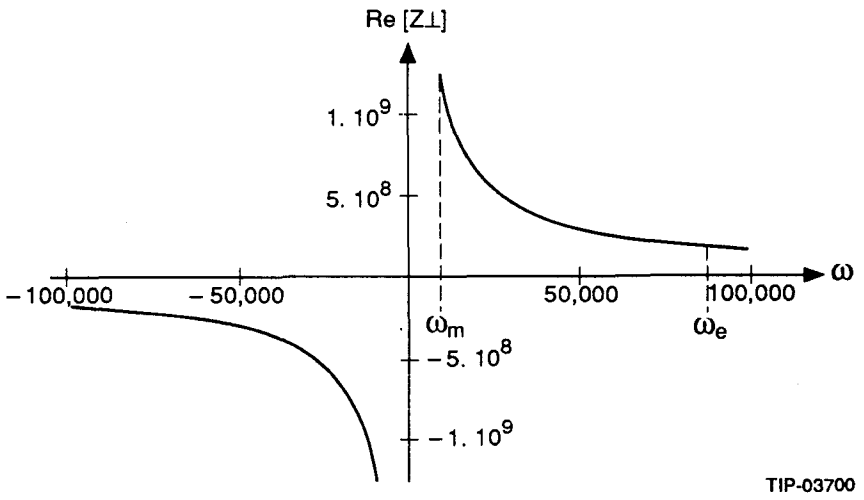

Figure 16. Resistive Wall Transverse Impedance at Low Frequency.

To perform the multibunch instability simulations, the time-dependent impedance is required. This can be obtained by making the inverse Fourier transformation of Eq. (11). However, even if an explicit expression were found, we would need to consider on the order of 10^8 interactions among the bunches per turn (due to the characteristics of this wake field). This approach would require hundreds of hours of CPU time for some hundred turns. Therefore, a different approach is required to study this case.

The first observation from Figure 16 is that the most important frequencies are those close to the zero frequency. For protons traveling in a collider machine with angular frequency ω_o, the frequencies of interest are

$$\omega_k = \omega_o(\Delta_\beta + k) \ , \tag{15a}$$

where Δ_β is the fractional part of the tune of the machine such that

$$-1/2 < \Delta_\beta < 1/2 \ . \tag{15b}$$

Each k corresponds to one possible multibunch mode of oscillation. This mode is stable for $k \geq 1$ and unstable for $k \leq -1$. The fundamental mode, $k = 0$, is unstable or stable depending on whether Δ_β is negative or positive. The second observation is that at this very low frequency the beam wall impedance looks like a resonator impedance. Hence, it can be approximated by this resonator impedance (see Figure 17), where the resonant frequency is the above-mentioned ω_k, the shunt impedance is just $Re[Z_\perp(\omega_k)]$, and the quality factor Q_o can be selected to approximate the shape of the resistive wall impedance. Therefore, the problem is reduced to the previous multibunch instability due to an rf system, and the above program can be applied using this new resonator impedance.

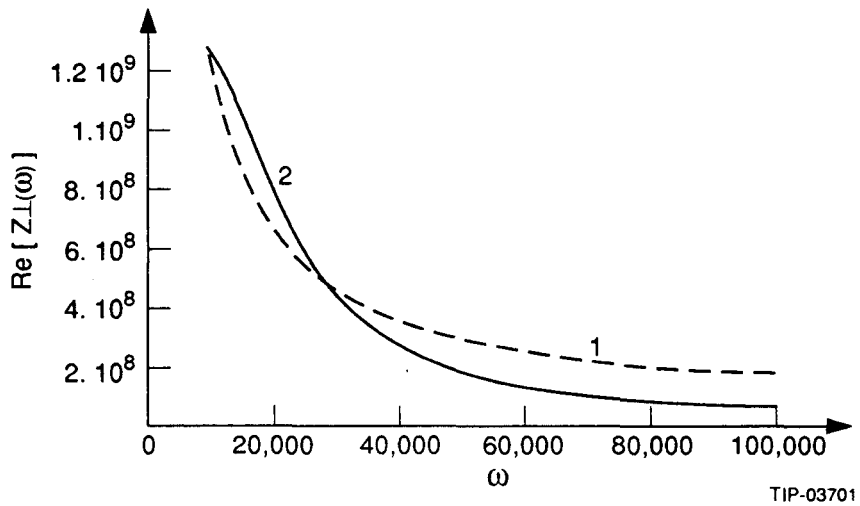

Figure 17. Comparison Between Resistive and Resonant Impedances.

The growth time of the instability and its dependence with the copper thickness will be estimated. Figure 18 shows the maximum amplitude as a function of the number of turns, obtaining a growth time of about 0.09 s $\left(\mathrm{D(j)=1}\right)$. Figure 19 shows how this growth time depends on the fractional part of the tune for three different thicknesses of copper. This figure indicates a clear benefit when the thickness of copper in the beam tube increases. For a copper thickness of 0.64 mm, the resistive wall instability is influenced only by the copper (for a fractional part of the tune between 0.1 and 0.9). This happens because, at the minimum value $\Delta_\beta = 0.1$, the resonant frequency ($\omega_m = |\Delta_\beta|\omega_o = 2.163$ kHz) coincides with the critical frequency, ω_c, which is such that the copper skin depth has the same value as the copper thickness at this frequency $\left(\delta_1(\omega_c) = 0.64 \text{ mm}\right)$. Higher value of copper thickness is almost irrelevant for the resistive wall instability. If for a copper thickness of 0.05 mm a maximum pressure of 0.646 atm is expected at the midplane of the beam tube during a main dipole quench,[13] the maximum pressure expected for a copper thickness of 0.1 mm, 0.3 mm, and 0.64 mm would be 1.29 atm, 3.87 atm, and 8.2 atm (18.94 psi, 56.81 psi, and 120.3 psi). The value of 8.2 atm is inside the tolerable values for a stainless steel thickness of 1 mm, and with a very wide safety margin for a thickness of 1.5 mm.[14]

The growth-time dependence with the quality factor Q_o will now be addressed. Figure 20 shows how the growth time depends on the quality factor Q_o, selected to fit the resistive wall impedance. The figure shows a variation of about 10% in the growth time for a variation of 400% in Q_o. Therefore, the result is not strongly dependent on the fitting parameter.

To verify that the instability is that of the resistive wall, the phase space of the bunches must be examined. Figure 21 shows the growth time for higher-order modes of multibunch oscillations. Figures 22–24 show the phase space generated by the bunches during the instability at some particular turn for the fundamental mode (Δ_β), and the next two higher-order modes ($\Delta_\beta - 1$ and $\Delta_\beta - 2$). As can be seen, they represent the expected phase space due to resistive wall instability.

Figure 25 shows the comparison of the simulations with the analytical approach (ZAP code) for several higher-order modes and two different materials, copper and stainless steel. (It is pointed out that ZAP code does not handle a stainless steel beam tube coated with copper.) From this figure, it is seen that the simulation results are very consistent with analytical results.

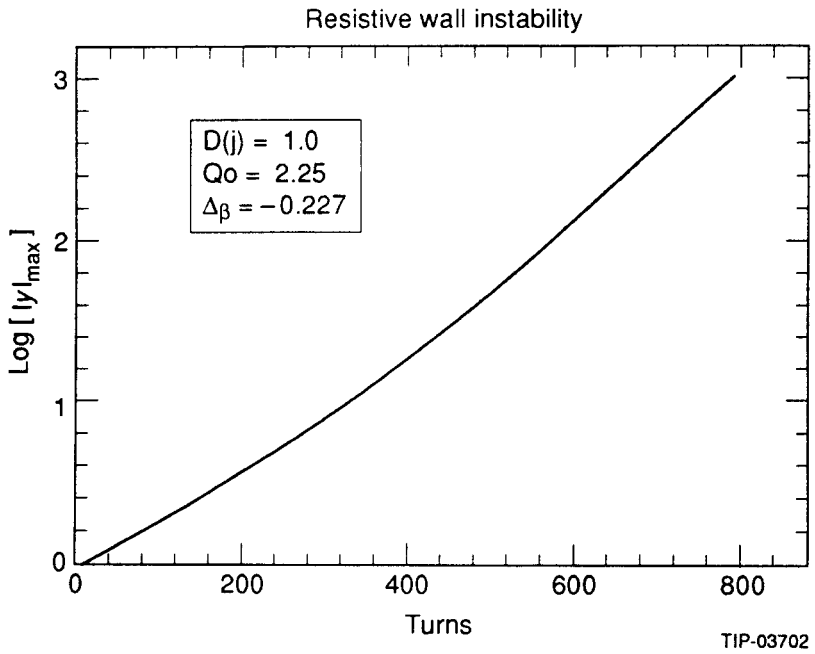

Figure 18. Maximum Amplitude Growth.

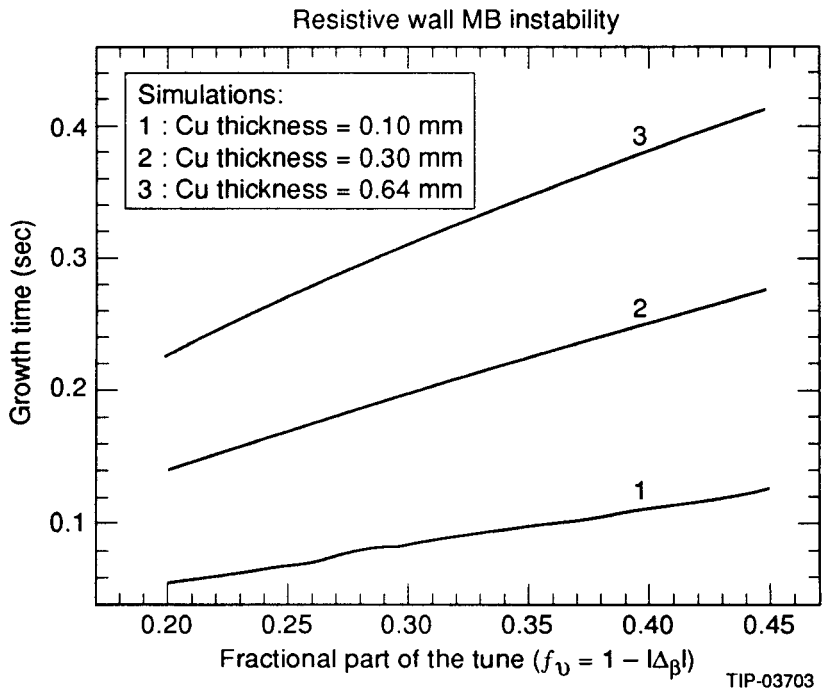

Figure 19. Beam Instability Growth Time as a Function of the Fractional Part of the Tune of the Collider and for Several Copper Thicknesses.

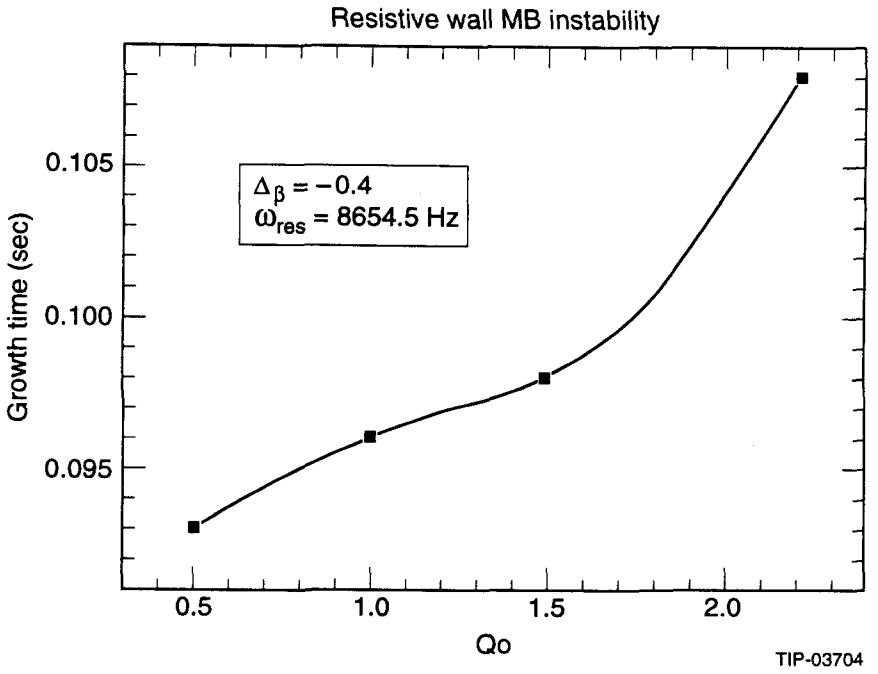

Figure 20. Beam Instability Growth Time-Dependence on the Quality Factor of the Resonant Impedance Approximation.

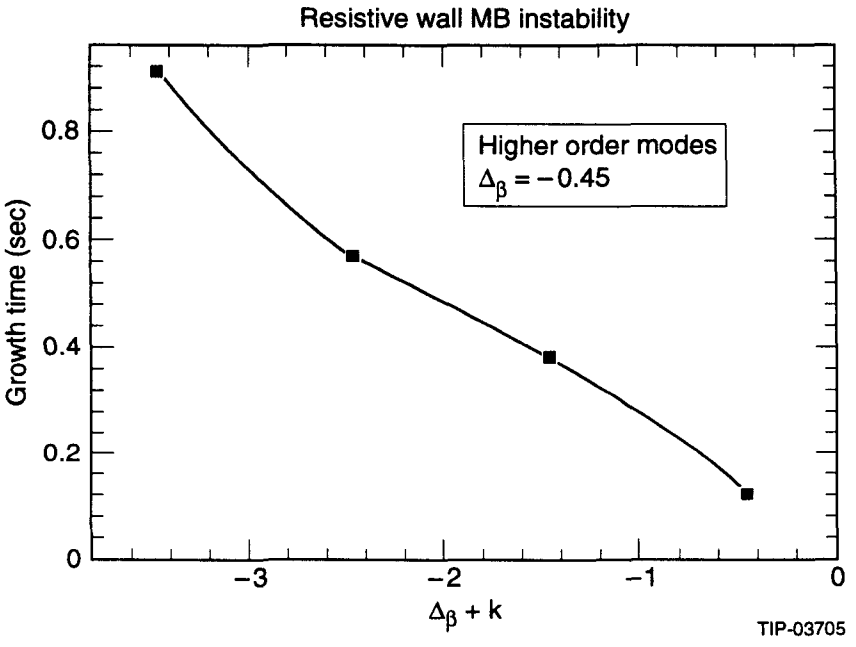

Figure 21. Beam Instability Growth Time for Higher-Order Modes.

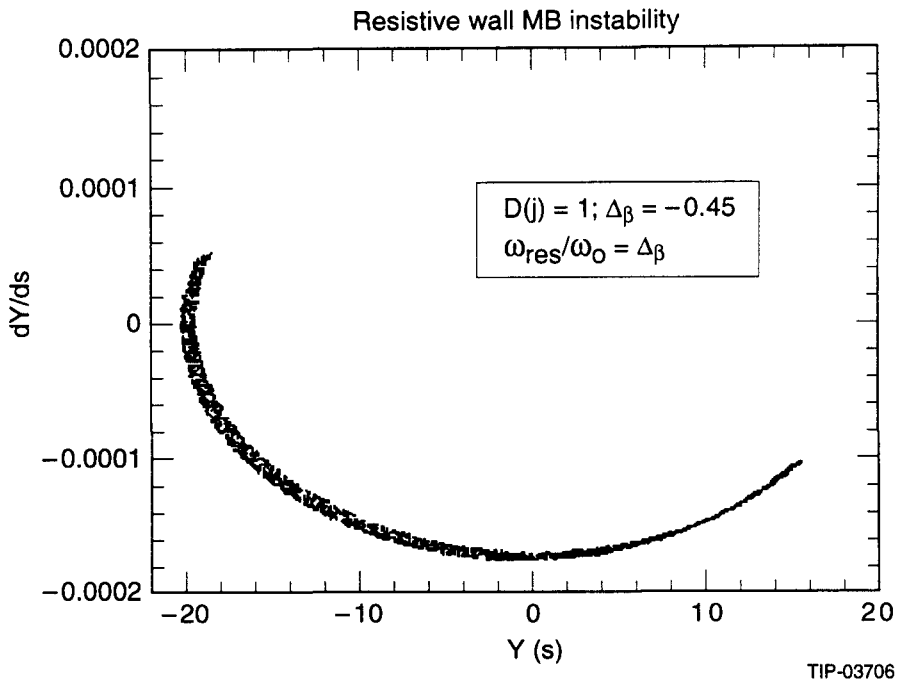

Figure 22. Beam Phase Space Induced by the Fundamental Mode Instability.

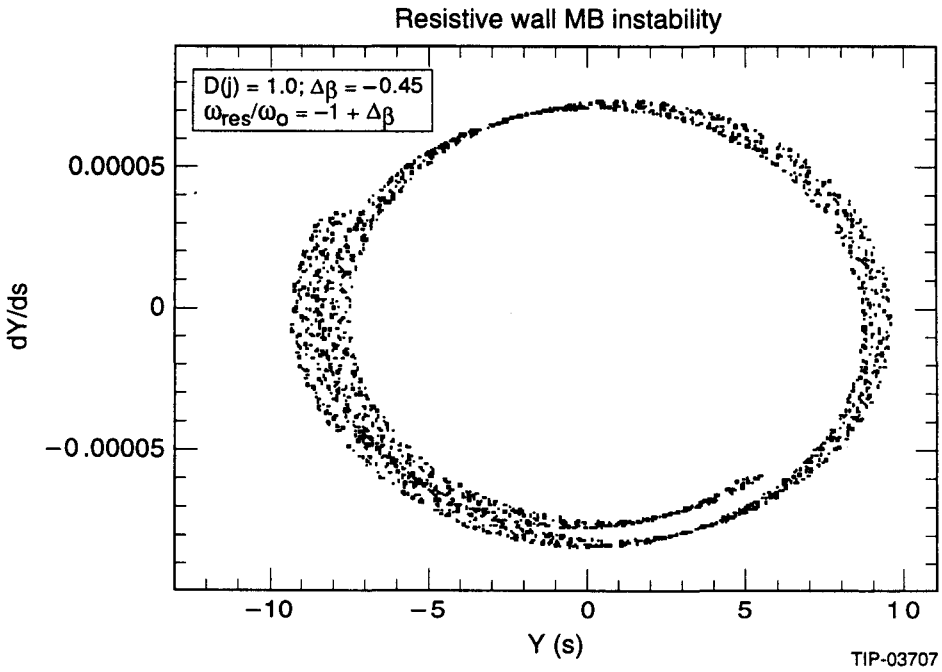

Figure 23. Beam Phase Space Induced by the First Higher-Order Mode Instability.

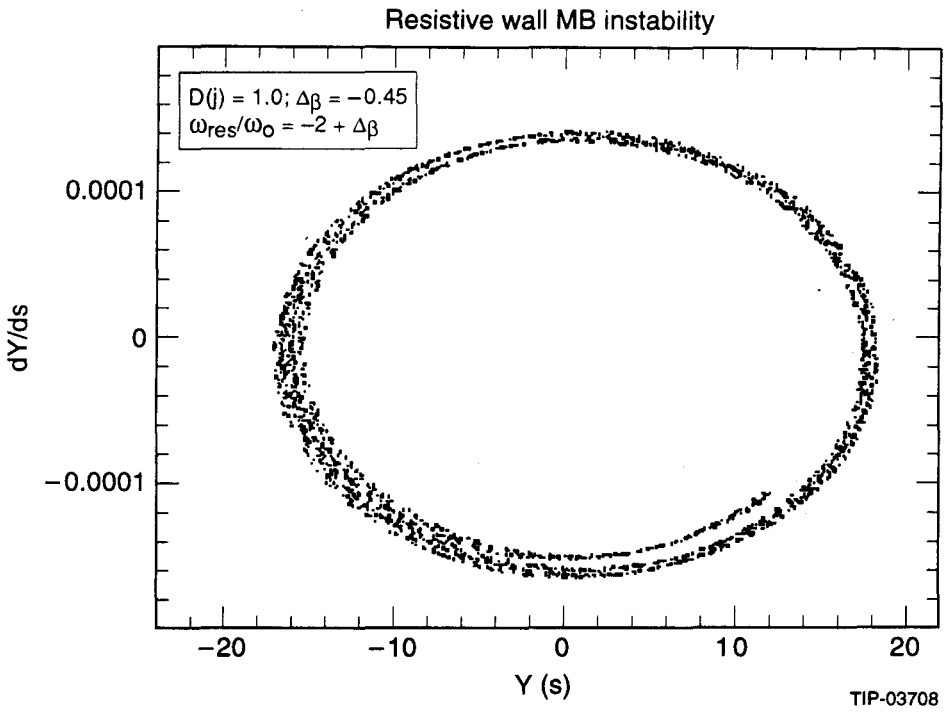

Figure 24. Beam Phase Space Induced by the Second Higher-Order Mode Instability.

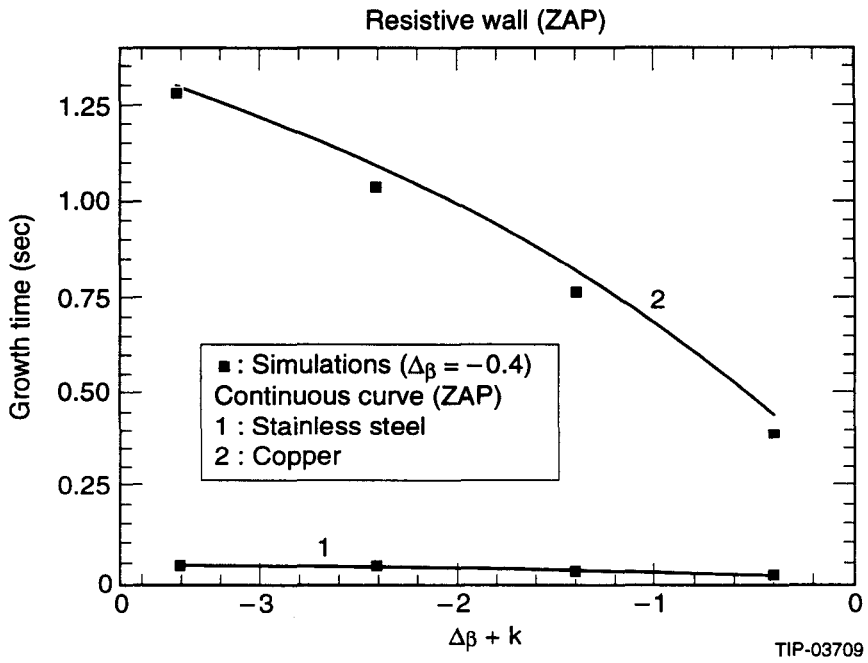

Figure 25. Simulations and ZAP Code Comparisons of the Instability Growth Time for Different Higher-Order Modes and Materials.

7.1 Single-Unit Feedback System for the Resistive Wall Instability

Using a single-unit feedback system (one BPM and one K with associated electronics) to correct the beam displacements, the procedure is the same as that seen in Section 5 but taking p turns average value of the displacements of the bunches at the BPM (p could be a rational number):

$$< Y >_p = \frac{1}{pM} \sum_{i=1}^{pM} Y_i^{BPM} , \tag{16}$$

that is, the correction to the trajectory of the particle changes every p-turns, and all the bunches receives the same correction proportional to $< Y >_p$, except for noise. This implies that the kicker flat-top time is

$$ft = p \times 2.904 \times 10^{-4} \text{ sec.} \tag{17}$$

The bandwidth (BW) of the feedback system will be assumed that one defined by the batch to batch separation (1.7 μs), BW$\geq$0.3 MHz.

Varying the parameters gain (g), noise (δY), and flat-top (p), the simulations indicate that this single-unit feedback system must be very strong to damp completely the instability for a copper thickness of 0.1 mm. Figure 26 shows the average displacement of the beam at the BPM as a function of the time (number of turns) for a feedback system with parameters: $g = 0.1$, $\delta Y = 10$ μm, $p = 2$, and $\Delta_\beta = -0.75$. The growth of the oscillations after 100 turns comes from the inability of the feedback system to damp entirely the instability. However, this single unit is able to damp the resistive wall instability for a copper thickness greater than 0.3 mm.

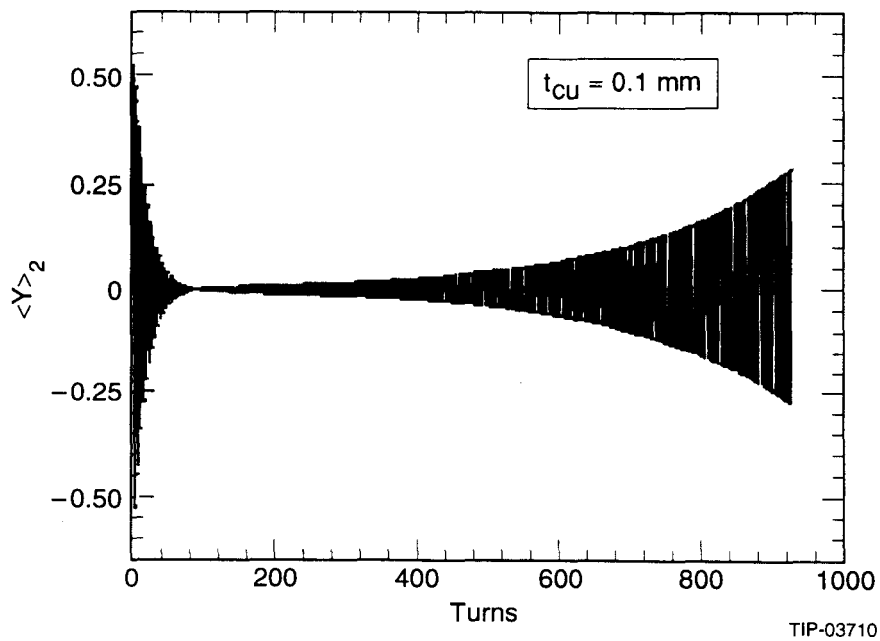

Figure 26. Two-Turns Average Value of the Beam Behavior with Single-Unit Feedback for a Copper Thickness of 0.1 mm.

Figures 27 and 28 show this damping effect for $g = 0.05$, $\delta Y = 100\ \mu$m, $p = 2$, and $\Delta_\beta = -0.75$. Table 2 summarizes most of the calculations made with the single-unit feedback system.

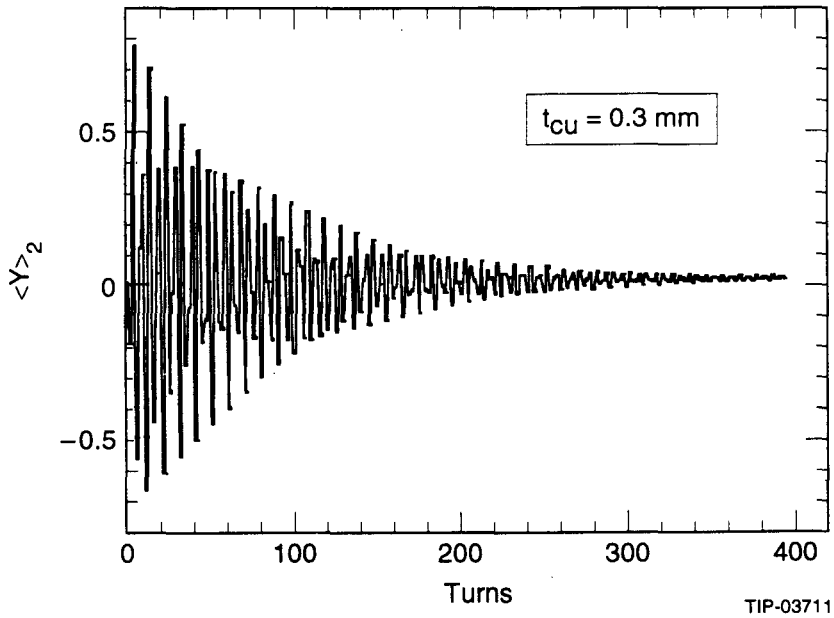

Figure 27. Two-Turns Average Value of the Beam Behavior with Single-Unit Feedback for a Copper Thickness of 0.3 mm.

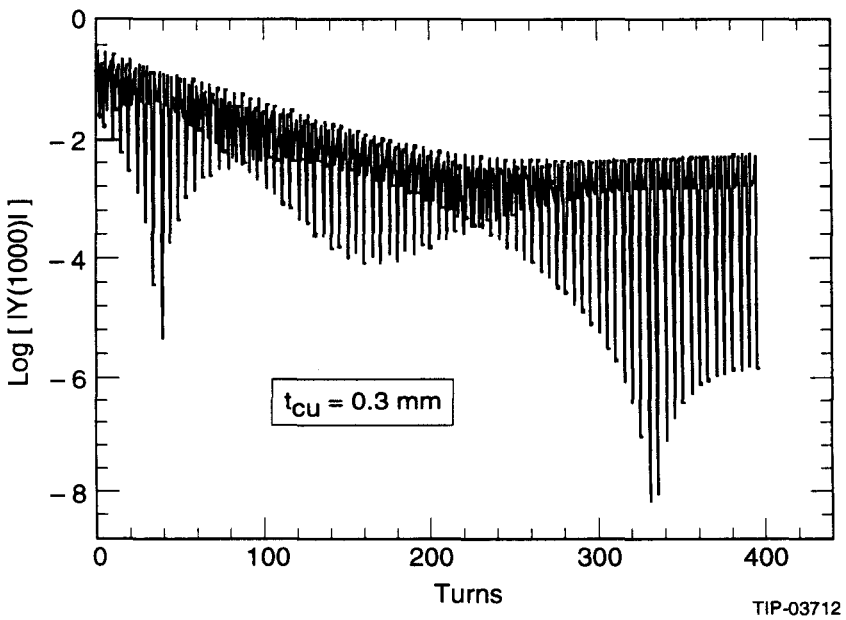

Figure 28. Amplitude Behavior of Bunch 1000 with Single-Unit Feedback for a Copper Thickness of 0.3 mm.

Table 2. Single-Unit Feedback System.[a]

$-1+\Delta_\beta = -0.75$			
Cu Thickness—t_1 (mm)	0.1	0.3	0.64
Growth Time[b]—τ (ms)	56	139	225
BPM Resolution—δY (μm)	≤ 100	≤ 500	same
Gain—g	≥ 0.30	≥ 0.01	same
flat-top—(p)	2	2	same

[a] stainless steel thickness $t_2 = 1.0$ mm
[b] without feedback system

7.2 Two-Unit Feedback System for the Resistive Wall Instability

Using a two-unit feedback system to correct the resistive wall instability affords more degrees of freedom. The units could be spatially separated or overlapped, as shown in Figure 29. The corresponding matrix transformations are more complicated than those in expressions (8) and are given, for the separated case, by

$$a(\mu_1) = \begin{pmatrix} \sqrt{\frac{\beta_{B1}}{\beta_R}}\cos\mu_1 & \sqrt{\beta_{B1}\beta_R}\sin\mu_1 \\ \frac{-(\sin\mu_1 + \alpha_{B1}\cos\mu_1)}{\sqrt{\beta_{B1}\beta_R}} & \sqrt{\frac{\beta_R}{\beta_{B1}}}(\cos\mu_1 - \alpha_{B1}\sin\mu_1) \end{pmatrix}, \tag{18a}$$

$$b = \begin{pmatrix} \alpha_{B1}\sqrt{\frac{\beta_{K1}}{\beta_{B1}}} & \sqrt{\beta_{K1}\beta_{B1}} \\ -\frac{1+\alpha_{K1}\alpha_{B1}}{\sqrt{\beta_{K1}\beta_{B1}}} & -\alpha_{K1}\sqrt{\frac{\beta_{B1}}{\beta_{K1}}} \end{pmatrix}, \tag{18b}$$

$$c(\mu_2) = \begin{pmatrix} \sqrt{\frac{\beta_{B2}}{\beta_{K1}}}(\cos\mu_2 + \alpha_{K1}\sin\mu_2) & \sqrt{\beta_{K1}\beta_{B2}}\sin\mu_2 \\ -\frac{1+\alpha_{K1}\alpha_{B2}}{\sqrt{\beta_{K1}\beta_{B2}}}\sin\mu_2 + \frac{\alpha_{K1}-\alpha_{B2}}{\sqrt{\beta_{K1}\beta_{B2}}}\cos\mu_2 & \sqrt{\frac{\beta_{K1}}{\beta_{B2}}}(\cos\mu_3 - \alpha_{B2}\sin\mu_2) \end{pmatrix}, \tag{18c}$$

$$d = \begin{pmatrix} \alpha_{B2}\sqrt{\frac{\beta_{K2}}{\beta_{B2}}} & \sqrt{\beta_{K2}\beta_{B2}} \\ -\frac{1+\alpha_{K2}\alpha_{B2}}{\sqrt{\beta_{K2}\beta_{B2}}} & -\alpha_{K2}\sqrt{\frac{\beta_{B2}}{\beta_{K2}}} \end{pmatrix}, \tag{18d}$$

and

$$e(\mu_3) = \begin{pmatrix} \sqrt{\frac{\beta_R}{\beta_{K2}}}(\cos\mu_3 + \alpha_{K2}\sin\mu_3) & \sqrt{\beta_R\beta_{K2}}\sin\mu_3 \\ -\frac{1}{\sqrt{\beta_R\beta_{K2}}}(\sin\mu_3 - \alpha_{K2}\cos\mu_3) & \sqrt{\frac{\beta_{K2}}{\beta_R}}\cos\mu_3 \end{pmatrix}, \tag{18e}$$

where the meaning of the subindex is clearly deduced from Figure 29 (a). The kicks provided by the kickers to the bunches are given by expression (7) but using the average value in expression (16). The first point to make is that the results do not depend much on the separation phase μ_2, as long as both feedback units are located in the dispersion-free region of the Collider. Although there is an improvement in the damping, the results indicate that the two-unit overlapped case seen in Figure 29(b) and (c) behaves very much like the one-unit case; *i.e.*, it is unable to damp the resistive wall instability generated by the copper thickness of 0.1 mm in the beam pipe. Therefore, this case will not be discussed further.

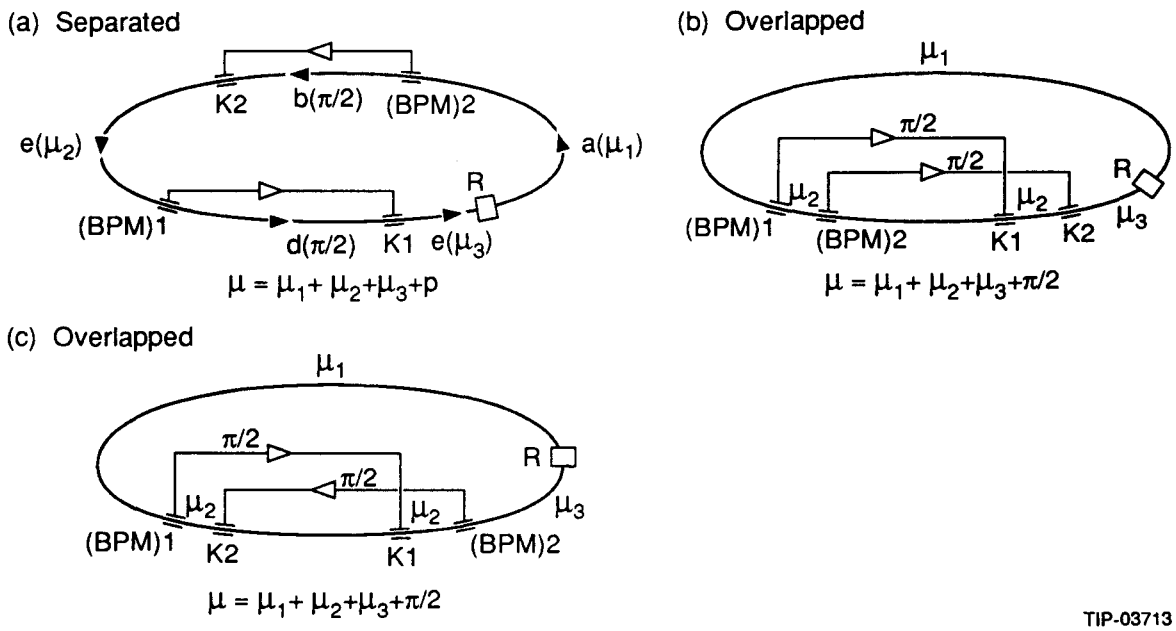

Figure 29. Two-Unit Feedback System Configurations.

Using the separated case (a), Figures 30 and 31 show the damping effect on the two-turns average value of the amplitude of the oscillations at (BPM)1 of Figure 29 and on the amplitude of bunch 1000. The characteristics of the feedback system of both units are the same as shown in these figures. Table 3 is a summary of the calculations.

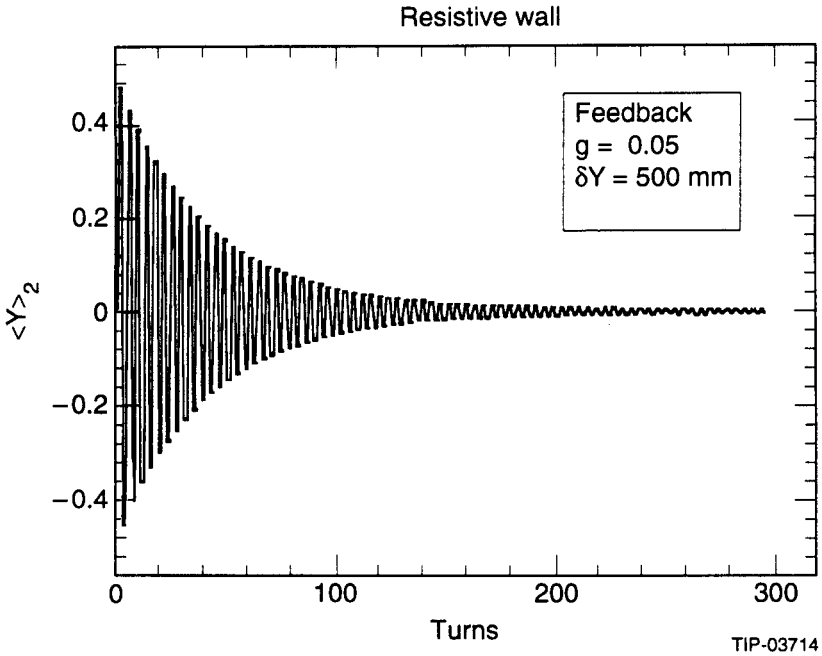

Figure 30. Two-Turns Average Value of the Beam Behavior with Two-Unit Separated Feedback System for a Copper Thickness of 0.1 mm.

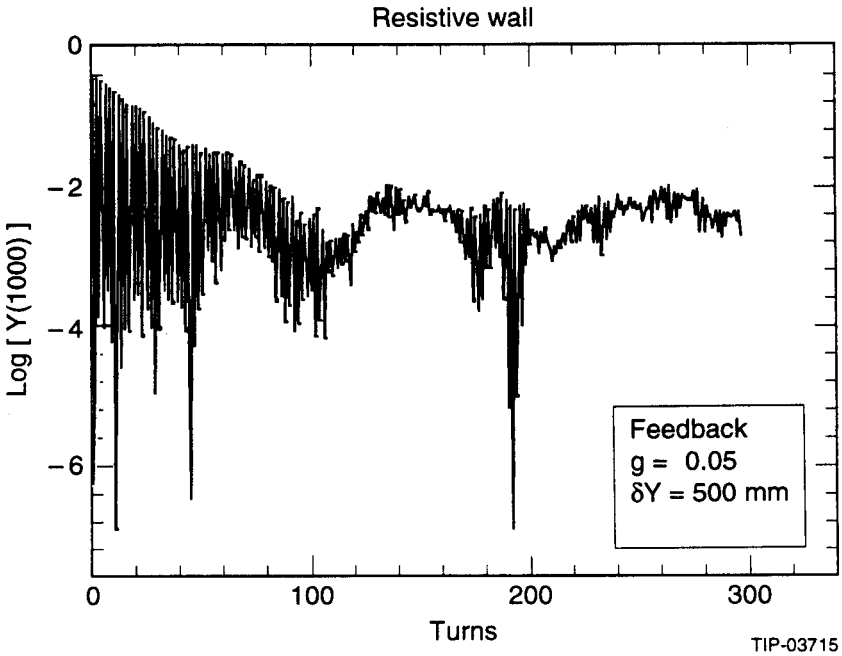

Figure 31. Amplitude Behavior of Bunch 1000 with Two-Unit Separated Feedback System for a Copper Thickness of 0.1 mm.

Table 3. Two-Independent-Unit Feedback System.[a]

$-1+\Delta_\beta = -0.75$			
Cu Thickness—t_1 (mm)	0.1	0.3	0.64
Growth Time[b]—τ (ms)	56	139	225
BPM Resolution—δY (μm)	≤ 500	≤ 1000	same
Gain—g	≥ 0.03	≥ 0.01	same
flat-top—(p)	2	2	same

[a] stainless steel thickness $t_2 = 1.0$ mm
[b] without feedback system

8.0 COMMENTS AND CONCLUSION

The transverse dipole-mode multibunch instability in the Collider due to an rf cavity and the resistive wall was simulated using the code TADIMMI.

For the rf cavity case the following results were obtained: Using a single PEP cavity, the resulting growth time is approximately 9 s for the symmetric filling case with uniform distribution, which is in good agreement with the analytical approach (ZAP code). The growth time is higher for the nonsymmetric case than for the symmetric case, which verifies the qualitative analytical approach. Killing some of the HOM of the PEP cavity does not help much to eliminate the dipole-mode multibunch instability. However, the De-Q and De-R/Q are very effective in increasing the growth time of this instability. A De-Q factor of 250 ($< R/Q > \sim 125\ \Omega/\mathrm{m}$) is good enough to overcome the instability even at higher luminosity. This same estimation indicates that a single-cell cavity with couplers may be the best option to control multibunch instability. Since $D(j)$ was taken as a random variable and can be associated with the product $D(j)R_\lambda/Q_\lambda$, the calculations also estimated the statistical effect on the impedance peak of the HOM of the cavity.[15] Finally, the feedback scheme designed for the Collider, whether a same-turn or previous-turn scheme, is able to damp completely the transverse dipole-mode instability. In summary, a safe control of the transverse dipole-mode multibunch instability due to the rf system is obtained using single-cell rf cavities (normal or s.c.) with HOM couplers (De-Q) and the feedback system.

For the resistive wall case, a resonant impedance approximation was made to the resistive wall impedance behavior at low frequency. This approximation allowed us to use the same computer program to estimate the growth time of the resistive wall multibunch instability. The results agree very well with the analytical approach, ZAP code for pure materials, copper, and stainless steel. (ZAP does not handle copper-coated tubes.) The resistive wall impedance expression and the resonant approximation indicate that a copper thickness greater than 0.64 mm does not have a significant effect on the beam instability. In addition,

the dipole quench analysis and the maximum allowable stress in the beam tube suggest that the value 0.64 mm is tolerable in the beam tube. The fast growth time of the resistive wall instability, approximately 0.1 s, allowed us to study the feedback system as a function of the noise levels and the gain of the system. The main result of these studies is that a single-unit feedback system would have to be very strong to kill the instability that arises because of a copper thickness of 0.1 mm (see Table 2). A feedback system one order of magnitude weaker can be obtained using a two-independent-unit feedback system (see Table 3). This better control of the resistive wall instability using two BPMs and two Ks was recently pointed out at Dubna (UNK).[16] Note that the restrictions on the BPM resolution in Tables 2 and 3 correspond to the control of the transverse dipole-mode multibunch instability. This noise is likely to blow up the emittance. To avoid emittance blow-up due to this feedback system, reduction of this BPM resolution by about two orders of magnitude may be required. (Work is in progress.)

One might think that if the aperture of the beam pipe were increased by a factor of approximately 1.5 and the liner were used, the resistive wall would not be a problem with 0.1 mm of copper thickness and a single-unit feedback system. However, this increment reduces the impedance by a factor of only 1/3.37, ((Eq.(11)), and the liner may increase the impedance by a factor of 2.5 since its operational temperature is 80 K, bringing about just a 25% reduction in the impedance. Moreover, upgrading the Collider to 10^{34} cm^{-2} sec^{-1} luminosity has the equivalent effect of a tenfold increase in the resistive wall interaction, making dubious the control of the instability with these elements. Therefore, a good control of the transverse dipole-mode multibunch instability due to the resistive wall can be obtained using a two-unit feedback system (two BPMs and two Ks with a gain $g = 0.03$) and a copper thickness of 0.3 mm in the beam pipe.

It is pointed out that for each BPM there may be another BPM$'$ associated with it and separated by a phase advance of $\pi/2$, which may be necessary for large changes in the correction signal phase due to changes in tune.[17] Since this BPM$'$ does not affect the beam dynamics, it has not been considered in the simulations. Finally, optimization analysis of the two BPM-two K feedback system is underway and will be reported in the near future.

ACKNOWLEDGEMENTS

We wish to thank Dr. A. Chao for many valuable discussions and suggestions, and Dr. R. Meinke, Dr. R. Gerig, and Dr. R. Schwitters for their support at the SSCL.

REFERENCES

1. SSCL-SR-1056, July 1990.
2. SSC-SR-2020, March 1986.
3. A. W. Chao, SLAC-PUB-2946, June 1982.
4. E. D. Courant and H. S. Snyder, Ann. of Phys. 3,1 (1958).
5. M. S. Zisman, S. Chattopadhyay, and J. J. Bisognano, "ZAP user's manual," LBL-21270 (1986).
6. R. D. Kohaupt, DESY 85-139, December 1985.
7. X. Wang, internal communication, 1992.
8. CERN 91-03, Section 8.3, May 1991.
9. S. van der Meer *et al., Phys. Report* **58**, 2, 73 (1980). D. Heins *et al.*, DESY 91-036, April 1991. R. D. Kohaupt *et al.*, DESY 89-157, November 1989.
10. W. Chao, internal communication, 1992.
11. V.A. Lebedev *et al.*, Novosibirsk 91-120, 1991.
12. A. Papoulis, *Probability, Random Variables, and Stochastic Processes*, McGraw-Hill, 1965, p. 266.
13. G. López, SSCL-295 (1991).
14. King-Yuen Ng and Jack Peterson, SSC-168 (1988).
15. T. Suzuki and K. Yokoya, *Nucl. Instrum. Methods* **203**, 45 (1982).
16. B. Sheldon, memorandum to SSCL, Sept. 30, 1992.
17. E. Raka, *Part. Accel.*, **27**, 21 (1990).
18. F. Sacherer, CERN/SI-BR/72-5 (1972).

APPENDIX A
PEP CAVITY

Table A.1 lists some characteristics of the 358.9-MHz PEP cavity.

Table A.1. Characteristics of the 358.9-MHz PEP Cavity.

λ	ω_λ (MHz)	R_λ ($M\Omega$/m)	Q_λ	$\left(\frac{R}{Q}\right)\lambda$ (Ω/m)	$\frac{2cQ_\lambda}{\omega_\lambda S_B}$
1	3179.29	1.57	47,100	33.33	1777
2	3982.28	1.81	62,700	28.86	1889
3	4865.69	17.32	48,500	357.11	1196
4	6078.35	2.30	98,400	23.37	1943
5	6854.95	5.78	41,500	92.04	1099
6	6873.80	12.28	41,500	295.90	724
7	7809.99	2.50	59,300	42.16	911
8	8589.11	13.37	67,300	198.66	940
9	10,090.79	3.41	62,800	54.29	747
10	10,662.56	6.71	63,500	105.67	714

APPENDIX B
SYMMETRIC AND NONSYMMETRIC ANALYTICAL APPROACH

For the symmetric case, suppose that all the degrees of freedom of the particle motion are uncoupled, and that all the bunches are equally spaced and uniformly distributed along the ring. If there are B bunches in the ring, the equation that governs the distribution of particles of the j-bunch due to the wake-field force of the other bunches, $F(f, x, v, t)$, is called the Vlasov's equation and can be written as

$$\frac{\partial f^j}{\partial t} + v\frac{\partial f^j}{\partial x} + F(f, x, v, t)\frac{\partial f^j}{\partial v} = 0 \quad \text{, for } \; j = 1, ..., B, \tag{B.1}$$

where $t, x, and\ v$ represent the time, the transverse bunch displacement, and the transverse bunch velocity, respectively, and f is the beam vector, $f = (f^1, \ldots, f^B)$. Because of the electromagnetic origin of the wake-field forces, F is a linear operator with respect to the beam vector.

This nonlinear couple-integral-differential equation is, in general, very difficult to solve. Therefore, the usual approach is to use a first-order perturbation in the density, *i.e.*, assume a bunch density of the form

$$f^j = f_o^j + y^j \exp(-i\Omega t) \ , \tag{B.2}$$

where f_o^j is the initial distribution and Ω is the coupled bunch frequency of oscillation. Substituting $(B.2)$ in $(B.1)$ and keeping first-order terms, the following equation is obtained:

$$-iv\frac{\partial y^j}{\partial x} - i\frac{\partial f_o^j}{\partial v}F(\vec{y}, \Omega) = \Omega y^j \quad j = 1, ..., B, \tag{B.3}$$

where the dependence of F on x and v has been ignored. In addition, assume that the frequency of oscillation is almost the same as the betatron frequency, ω_β, so that we can substitute this frequency on the left-hand side of $(B.3)$; then, the following eigenvalue equation results:

$$L(\vec{y}) = \Omega\vec{y} \ , \tag{B.4}$$

where L, the Sacherer's operator,[18] can be expressed in the following way:

$$L = -iv\frac{\partial}{\partial x} - i\frac{\partial f_o^j}{\partial v}F(\ , \omega_\beta) \ . \tag{B.5}$$

The solutions of $(B.4)$ bring about the eigenmode couple bunch oscillations of the beam. The imaginary part of the eigenvalue gives the growth rate of the multibunch motion,

$$\tau = \frac{1}{Im(\Omega)} \ , \tag{B.6}$$

which is unstable if this is positive. In this case, τ is called the growth time of the unstable mode. This solution must satisfy the requirement of being a small perturbation, *i.e.*,

$$|y^j \exp(Im(\Omega)t)| \leq |f_o^j| \ , \tag{B.7}$$

which also give us the maximum time for the approximation to be valid. For a time longer than this, the solution (and the whole approach) may be meaningless.

For the nonsymmetric case, we can make the same assumptions as above. So, there are B bunches uniformly distributed along a ring, and the behavior of the bunches is described by the Sacherer equation (B.4), which clearly depends on the number of bunches. Each density function y^j is proportional to the number of particles in the bunch. Thus, the set of beam vectors

$$M = \{\vec{y}\} \ , \tag{B.8}$$

such that

$$\vec{y} = \begin{pmatrix} y^1 \\ \vdots \\ y^B \end{pmatrix} \ , \tag{B.9}$$

forms a vector space of dimension B over the complex number (in general). In this vector space it is possible to define an inner product

$$< \vec{y}_1 | \vec{y}_2 >= \int \vec{y}_1^{+}(\xi) \cdot \vec{y}_2(\xi) \ d\mu(\xi) \ , \tag{B.10}$$

where ξ represents the variables of integration and $\mu(\xi)$ is a measure in this space, and $+$ represents the adjoint operation. With this inner product, the set of eigenvectors, $\{\vec{y}_k, \ k = 1, ..., B\}$, of the linear equation (B.3),

$$L(\vec{y}_k) = \lambda_k \vec{y}_k \ , \tag{B.11}$$

can be chosen to be a orthonormal set,

$$< \vec{y}_k | \vec{y}_n >= \delta_{kn} \ . \tag{B.12}$$

Therefore, any vector, $\vec{y}$, of the space M can be expressed as a linear superposition of this orthonormal set:

$$\vec{y} = \sum_{k=1}^{B} c_k \vec{y}_k \ , \tag{B.13}$$

where c_k, k=1,...,B are complex numbers. The norm in this space can be defined through the inner product as

$$||\vec{y}|| = \sqrt{< \vec{y} | \vec{y} >} = \sqrt{\sum_{k=1}^{B} |c_k|^2} \ . \tag{B.14}$$

Assume now that the vector space is divided into two vector subspaces V and W. If $L_V = L|_V$, $L_W = L|_W$ are the restrictions of the linear operator L to these spaces, they are invariant spaces of these operators; *i.e.*, $L_V(V) \subseteq V$ and $L_W(W) \subseteq W$.

In addition, if $\vec{v}_n$ and $\vec{w}_m$ are eigenvectors associated with the operators L_V and L_W,

$$L_V(\vec{v}_n) = \gamma_n \vec{v}_n \quad , \tag{B.15}$$

and

$$L_W(\vec{w}_m) = \eta_m \vec{w}_m \ , \tag{B.16}$$

these vectors turn out to be orthogonals, $< \vec{v}_n | \vec{w}_m >= 0$. Therefore, the vector space M is the direct sum of the two orthogonal vector subspaces, $M = V \oplus W$, and the vector

$$\vec{y}_{vw} = \begin{pmatrix} \vec{v}_n \\ \vec{w}_m \end{pmatrix} \tag{B.17}$$

is a vector in the M space. Thus, it can be written as

$$\vec{y}_{vw} = \sum_{k=1}^{B} \alpha_k^{nm} \vec{y}_k \ . \tag{B.18}$$

Applying the operator L to the left- and right-hand sides of $(B.18)$, it follows that

$$L(\vec{y}_{vw}) = \begin{pmatrix} L_V(\vec{v}_n) \\ L_W(\vec{w}_m) \end{pmatrix} = \begin{pmatrix} \gamma_n \vec{v}_n \\ \eta_m \vec{w}_m \end{pmatrix} = \sum_{k=1}^{B} \alpha_k^{nm} \lambda_k \vec{y}_k \ . \tag{B.19}$$

Consequently, the product $< \vec{y}_{vw} | L(\vec{y}_{vw}) >$ is given by

$$\gamma_n \|\vec{v}_n\|_V^2 + \eta_m \|\vec{w}_m\|_W^2 = \sum_{k=1}^{B} |\alpha_k^{nm}|^2 \lambda_k \ , \tag{B.20}$$

where the norm in the vector subspaces is understood. similarly, as relation $(B.14)$, and the relation $(B.12)$ has been used.

Assume now a partial filling ring, $\vec{w}_m = \vec{0}$. From the definition of relation $(B.18)$ and relation $(B.11)$, it follows that

$$\|\vec{y}_{vw}\|^2 = \|\vec{v}_n\|_V^2 = \sum_{k=1}^{B} |\alpha_k^n|^2 \ . \tag{B.21}$$

Substituting this result in relation $(B.20)$, we get

$$\gamma_n = \frac{1}{\sum_{k=1}^{B} |\alpha_k^n|^2} \sum_{k=1}^{B} |\alpha_k^n|^2 \lambda_k \ . \tag{B.22}$$

This is the Kohaupt's result,[6] which relates the eigenvalues of the symmetric filling case with the eigenvalues of the asymmetric filling case through nonnegative real numbers, $|\alpha_k^{n0}|^2$. From this expression it is possible to give the following qualitative result. For any k and n,

1) If M is stable $(Im(\lambda_k) \leq 0) \Rightarrow V$ is also stable.

2) If V is stable $(Im(\gamma_n) \leq 0) \not\Rightarrow M$ is stable.

In other words, the symmetric case represents the worst-case scenario for multibunch instabilities due to any type of wake-field source.